LIQUID METAL MHD FLOWS IN CIRCULAR DUCTS AT INTERMEDIATE HARTMANN NUMBERS AND INTERACTION PARAMETERS

MOLOKOV, S.[1], REED, C.B.[2]
[1]*Coventry University, School of Mathematical and Information Sciences, Priory Street, Coventry CV1 5FB, United Kingdom, e-mail: s.molokov@coventry.ac.uk*
[2]*Argonne National Laboratory, 9700 South Cass Avenue, Argonne, IL 60439, USA, e-mail: cbreed@anl.gov*

Abstract: Magnetohydrodynamic (MHD) flows in circular ducts in nonuniform magnetic fields are studied with reference to liquid metal blankets and divertors of fusion reactors. Flows in small and medium size reactors are characterized by moderate and low values of the Hartmann number (~50-2000) and the interaction parameter (~0.1-1000). The validity of the high-Hartmann number flow model for the intermediate range is discussed and the results of theoretical and experimental investigations are presented.

1. Introduction

Liquid metal flows in circular ducts play a fundamental role in liquid metal blankets and divertors for fusion reactors. Concerning blankets, both inlet and outlet pipes have circular cross-section. The flow in these pipes is fully three-dimensional, since liquid metal flows in a strong, nonuniform magnetic field. Similar situations occur in circular ducts supplying liquid metal to divertors elements [1], [2].

When a liquid metal flows in a strong magnetic field, electric currents are induced. These currents in turn interact with the magnetic field and the resulting electromagnetic force induces a high MHD pressure drop and significant nonuniformities of the velocity profile in the duct cross-section. The pressure drop in particular is considered to be one of the most critical issues for self-cooled blankets. If duct walls are electrically conducting, the magnitude of the electromagnetic force with respect to viscous and inertial forces is determined by two parameters, the Hartmann number, $Ha = a^* B_0^* (\sigma/\rho\nu)^{1/2}$, and the interaction parameter, $N = a^* \sigma B_0^{*2} / \rho v_0^*$, respectively. For insulating ducts a more appropriate measure of the importance of inertial effects is parameter *Ha/Re*, where $Re = a^* v_0^* / \nu$ is the Reynolds number. The range of parameter values for various machines, is shown in Table 1.

In the above, a^* (the duct radius), v_0^* (average fluid velocity), B_0^* is the characteristic value of the magnetic field, σ, ρ, ν are the electrical conductivity, density and kinematic viscosity of the fluid, respectively.

As the three-dimensional effects in blanket/divertor elements are of considerable importance, they have been studied very extensively in the past. Flows in straight circular ducts in a fringing field have been studied recently in [4]-[15] both theoretically and experimentally. For earlier references and for those on circular duct expansions, bends, etc. see reviews in [16]-[19].

Table 1. *Range of parameter values N, Ha, and Re in various tokamaks*

	ITER, ARIES	**C-MOD**	**NSTX**
Hartmann number, *Ha*	~10^3-10^5	~500-1000	~50-500
Interaction parameter, *N*	~10^3-10^5	~50-10^4	~0.1-1
Reynolds number, *Re*	~10^4-10^5	~10^4-10^5	~10^4-10^5
Ha/Re	~0.1	~0.03	~0.003
Most likely flow regimes for insulating ducts	Laminar MHD	Laminar, weakly turbulent MHD	Turbulent MHD

Most theoretical investigations have been performed using an asymptotic, high-*Ha* model. The model has shown excellent agreement with the experiments for ducts with thin conducting walls and for *N* as low as 600 [10].

Recently, however, the emphasis in the US has shifted to smaller experimental reactors, such as NSTX and C-MOD. Flows in NSTX will be clearly turbulent (Table 1), and thus very difficult to model (see Conclusions in [20]). On the other hand, duct flows in C-MOD are expected to be laminar, or maybe weakly turbulent in the lower end of *N*-values. Concerning the latter reactor, the question arises as to the range of applicability of the high-*Ha* model at intermidiate values of *Ha* and *N*, i.e. 10^2-10^3.

We address this issue in this investigation. We also estimate the importance of three-dimensional effects for the above-mentioned values of parameters. Theoretical results on inertialess flows in insulating ducts for $Ha = 10^2$ and $Ha = 10^3$ are presented in Sec. 4. Then comparison of the high-Ha model with the experiments on conducting ducts is made in Sec. 5.

2. Formulation

Consider a flow of a viscous, electrically conducting, incompressible fluid in a straight, circular duct in the *x*-direction (Fig. 1). Both the flow geometry studied here and the Cartesian co-ordinate system (*x*, *y*, *z*) are shown in the figure. Cylindrical co-ordinates (*r*, θ, *x*) are also used, which are defined as follows: $z = r\sin\theta$, $y = r\cos\theta$. The magnetic field $\mathbf{B}^* = B_0^* B(x,z)\hat{\mathbf{y}}$ is supposed to have a single component, out of the plane of the figure, where B_0^* is the characteristic value of the magnetic field in the upstream region, i.e. for $x \to -\infty$. Dimensional quantities are denoted by letters with asterisks, while their dimensionless counterparts - with the same letters, but without the asterisks.

The family of the magnetic fields studied here is $B(x) = \frac{1}{2}(B_d + B_u) + \frac{1}{2}(B_d - B_u)\tanh\gamma x$. The field induction varies between the constant values of $B_u = 1$ to the left of Line 1 and B_d to the right of Line 2 (see Fig. 1). The field is nonuniform between these lines. The field gradient is defined by γ. For γ = 0.8 the field approximates that in the ALEX facility [10].

The characteristic values of the length, the fluid velocity, the electric current density, the electric potential, the pressure and time are a^*, v_0^*, $\sigma v_0^* B_0^*$, $a^* v_0^* B_0^*$, $a^* \sigma v_0^* B_0^{*2}$, and a^*/v_0^* respectively. Then the dimensionless, inductionless equations governing the flow are [18]:

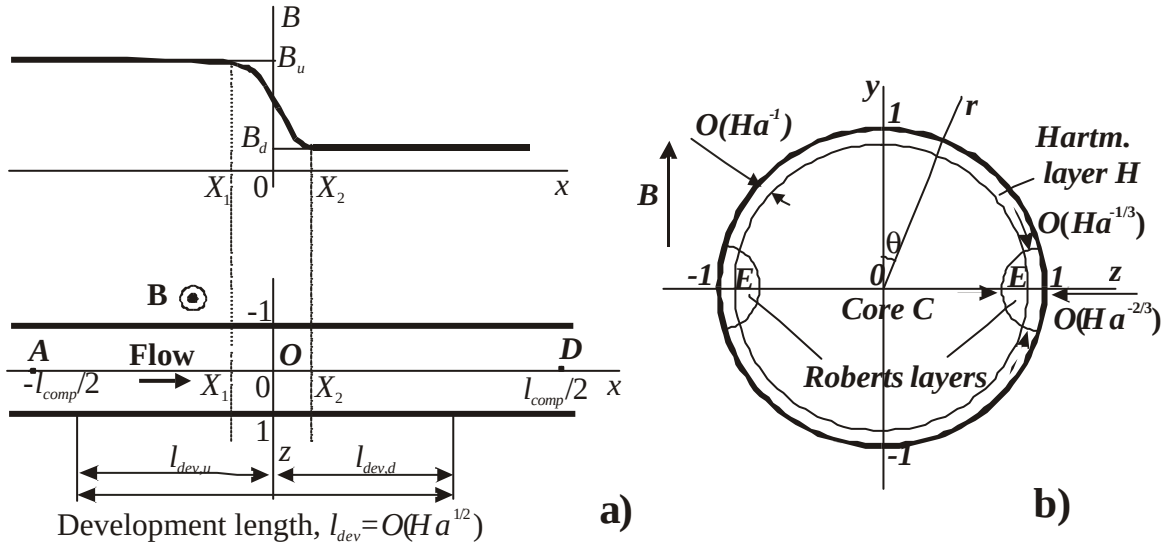

Fig. 1 *Schematic diagram of flow in a circular duct in a nonuniform magnetic field: a) magnetic field and the duct cross-section in the (x,z)-plane; b) duct cross-section in the (y,z)-plane, flow subregions at high Ha and the cylindrical co-ordinate system.*

$$Ha^{-2}\nabla^2\mathbf{v} + \mathbf{j}\times\mathbf{B} = \nabla p + N^{-1}\left[(\mathbf{v}\cdot\nabla)\mathbf{v} + \partial\mathbf{v}/\partial t\right], \quad \mathbf{j} = -\nabla\phi + \mathbf{v}\times\mathbf{B}, \qquad (1a,b)$$

$$\nabla\cdot\mathbf{v} = 0, \quad \nabla\cdot\mathbf{j} = 0, \qquad (1c,d)$$

where **v** is the fluid velocity, **j** is the electric current density, ϕ is the electric potential, p is the pressure, and t is time.

The boundary conditions at the duct wall are the no-slip- and the thin-wall- conditions [18]:

$$\mathbf{v} = 0, \quad j_r = -c\left[\frac{\partial^2\phi}{\partial x^2} + \frac{\partial^2\phi}{\partial\theta^2}\right] \quad \text{at } r = 1, \qquad (1e)$$

where j_r is the radial component of current.

Far upstream and far downstream the flow is supposed to be fully developed, which requires

$$\partial p/\partial z \to 0, \quad \partial\phi/\partial x \to 0 \quad \text{as } x \to \pm\infty. \qquad (1f,g)$$

Finally, the solution is normalized using the condition of a fixed average velocity:

$$2\int_{-\pi/2}^{\pi/2} d\theta \int_0^1 rudr = \pi, \qquad (1h)$$

where u is the x-component of velocity.

3. High-*Ha* flow model

In a sufficiently strong magnetic field the flow becomes inertialess, while the flow region splits into the following subregions (Fig. 1): the core C, the Hartmann layer H of thickness $O(Ha^{-1})$ at the wall, and passive Roberts layers E with dimensions $O(Ha^{-1/3})\times O(Ha^{-2/3})$ at $\theta = \pm\pi/2$, $r = 1$. The details of the high-*Ha* model, valid for terms up to $O(Ha^{-1})$ are omitted here. The analysis leads to two two-dimensional partial differential equations for the core pressure $P(x,z)$ and the wall electric potential $\Phi(x,z)$ as follows:

$$a_{11}\frac{\partial^2 P}{\partial x^2} + a_{22}\frac{\partial^2 P}{\partial\theta^2} + a_1\frac{\partial P}{\partial x} + a_2\frac{\partial P}{\partial\theta} + b_1\frac{\partial\Phi}{\partial x} + b_2\frac{\partial\Phi}{\partial\theta} = 0, \qquad (2a)$$

$$c_{11}\frac{\partial^2\Phi}{\partial x^2} + c_{22}\frac{\partial^2\Phi}{\partial\theta^2} + c_1\frac{\partial\Phi}{\partial x} + c_2\frac{\partial\Phi}{\partial\theta} + d_1\frac{\partial P}{\partial x} + d_2\frac{\partial P}{\partial\theta} = 0, \qquad (2b)$$

where coefficients c_{ij}, a_{ij}, b_i, d_i are functions of θ, x, Ha, and c. These equations, subject to appropriate boundary conditions, have been solved numerically on a non-equidistant grid using a finite-difference method as described in [13], [14]. The code, developed originally for insulating ducts, has been extended to include finite wall conductance.

4. Inertialess flow in an insulating duct

For very high magnetic fields the flow is inertialess. For an insulating duct this requires $N >> Ha^{1/2}$ [4].

Since $B_u \neq B_d$, for any fixed value of $z \neq 0$ there is a difference in the values of potential upstream and downstream. This axial potential difference drives axial electric currents and causes the three-dimensional effects.

The interaction of the magnetic field with the axial current pushes the fluid from the center of the duct to the sides in the upstream region, and peaks of axial velocity appear at the side regions (Fig. 2). The development of the axial velocity profiles at $y = 0$ along the duct

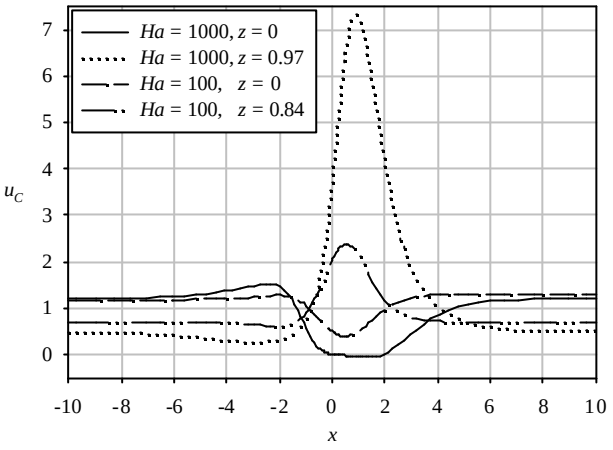

Fig. 2 *Inertialess flow in an insulating duct: axial velocity at y = 0 for different values of z and for Ha = 1000 and Ha =100.*

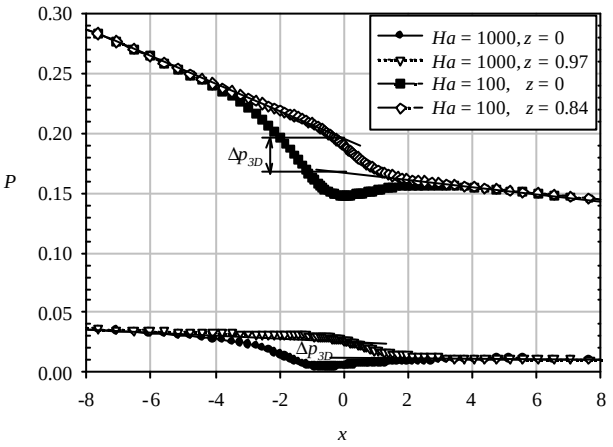

Fig. 3 *Inertialess flow in an insulating duct: variation of pressure with x at the center of the duct and near z = 1 for Ha = 1000 and Ha = 100, and the three-dimensional pressure drop.*

axis and at the side region for Ha = 1000 and for Ha = 100 is shown in Fig. 2. Since the fluid is pushed towards the side regions, a zone with reduced velocity develops in the center of the duct (Fig. 2). The flow in this zone is stagnant for Ha = 1000.

For Ha =1000 the development lengths in the upstream and the downstream regions are: $l_{dev,u}$ = 9.5 and $l_{dev,d}$ = 7.5, respectively. Thus the total development length is l_{dev} = 17 duct radii.

The development of the core pressure along the duct axis and in the side region for Ha = 1000 and for Ha = 100 is shown in Fig. 3. For Ha = 1000 the pressure values deviate from the fully developed ones in the region $-6 \le x \le 3$ owing to the three-dimensional effects. There is a partial pressure recovery at z = 0 in the region $-0.5 \le x \le 3$ owing to the returning current.

The three-dimensional pressure drop Δp_{3D}, defined in [13], [14] and shown in Fig. 3, is $1.48 \cdot 10^{-2}$ for Ha = 1000 and $4 \cdot 10^{-2}$ for Ha = 100, respectively. This gives the respective values of the three-dimensional length d_{3D} [13], [14], of 12.5 and 3.4. This means that for Ha = 1000 the three-dimensional effects are significant, while for Ha = 100 they can be neglected.

5. Conducting duct

The theoretical results obtained with the high-Ha, inertialess flow model have already shown a very good agreement with the experiments [10] for N as low as 600. The model used has been developed in [9] for $c >> Ha^{-1}$. Strictly speaking, it is valid for $Ha = \infty$. On the other hand, Hua & Walker [7] developed a flow model for insulating ducts, i.e. for a finite Hartmann number. Here we use the model defined by Eqs. (2), which is valid for both insulating and conducting ducts. Thus it may be viewed as a combined model of [9] and [7]. A similar approach has been used in [12], where various three-dimensional flows have been analysed.

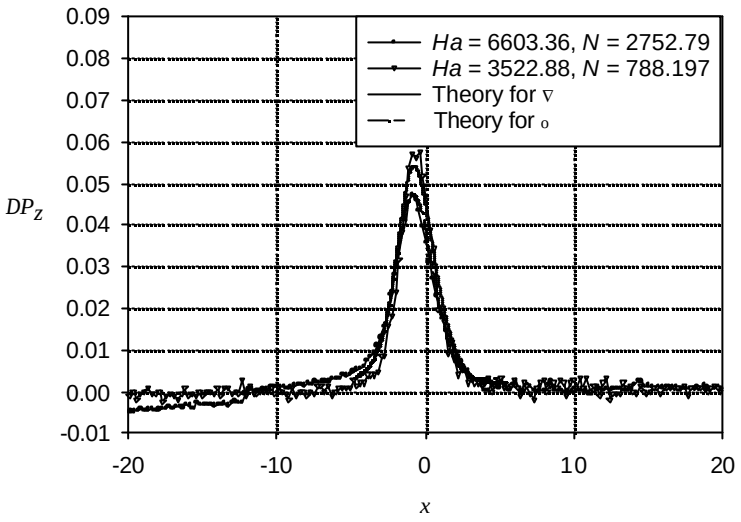

Fig. 4. *Transverse pressure difference $\Delta p_z = p(z=1) - p(z=0)$ in a conducting duct for two sets of parameters.*

Theoretical results have been compared with many experimental data obtained in the ALEX facility but not reported in [10]. Here only a brief summary is given.

In the experiments the wall conductance ratio was $c = 0.026$, the liquid metal, NaK at room temperature. Measured quantities included wall voltages, both axial and transverse pressure and local velocity from a LEVI probe. Data in the fringing region of the magnet were collected by moving the magnet with respect to the duct. Details of the experiment can be found in [21].

The results for transverse pressure differences ($\Delta p_z = p(z=1) - p(z=0)$) for two sets of parameters are shown in Fig. 4. In the nonuniform field region the approximation for both sets of parameters is very good. For $N = 788$ the peak of Δp_z is slightly underestimated. Similar type of agreement have been obtained for a wide range of parameter values of N and Ha.

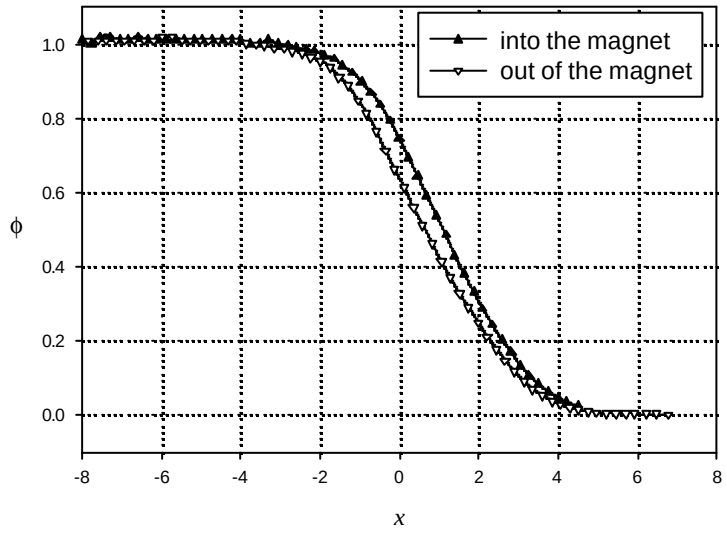

Fig. 5 *Experimental data for wall potential in a conducting duct at z = 1, y = 0 for Ha = 3077, N = 610.8*

The scatter of datapoints for $|x| > 10$ is the result of measuring a quantity which is essentially zero. Another reason might be the effect of inertia in the region of weak field.

To get a feeling of the importance of inertia, experimental data for wall potential at $y = 0$, $z = 1$ for flow into and out of the magnet have been plotted in Fig. 5. It is seen that there is a certain difference between these values. Concerning even lower values of $N \sim 50$-100, inertial effects will be very significant [5].

The high-Ha model breaks down when the local Hartmann number and interaction parameter defined by a local value of the field at a certain x are low. In these regions, at some distance from the magnet poles, the flow may be

highly inertial and even turbulent. These effects are being currently investigated using a CFX-based MHD code, which takes inertia into account. The results will be reported in the near future.

6. Conclusions

For values of *Ha* relevant to C-MOD the three-dimensional effects in insulating circular ducts in a nonuniform magnetic field are expected to be of considerable importance. The three-dimensional pressure drop is equivalent to the extension of ducts with fully developed flow by 12 duct radii. The nonuniformity of the fluid velocity is significant as well with velocity peaks reaching the value of about 7 times the average one. The development length resulting from the nonuniform field is about 17 duct radii. This means that the three-dimensional effects from various blanket/divertor elements may overlap, and the whole device may need to be treated as a single piece. Nevertheless, owing to much lower Hartmann numbers, three-dimensional effects in C-MOD will be less important than in large-scale machines, such as ARIES.

The high-*Ha* model may well be used to predict flows in conducting ducts for intermediate values of *Ha* and *N*. Inertial effects at the entrance to and exit from the magnet are being studied.

7. Acknowledgement

This work has been supported by the Office of Fusion Energy Sciences, U.S. Department of Energy, under Contract No. W-31-109-ENG-38.

8. References

[1] MATTAS, R., et al., (2000) *Fus. Eng. Des.* **49-50**, 127-134.
[2] KARASEV, B.G., TANANAEV, A.B. (1990) *Plasma Devices and Operations* **1**, 11-30.
[4] HOLROYD, R., WALKER, J.S. (1978) *J. Fluid Mech.* **84**, 471-495.
[5] HOLROYD, R. (1980) *J. Fluid Mech.* **96**, 355-374.
[6] WALKER, J.S. (1986) *J. Fluid Mech.* **167**, 199-217.
[7] HUA, T.Q., WALKER, J.S. (1989) *Int. J. Engng Sci.* **27,** 1079-1091.
[8] HUA, T.Q., PICOLOGLOU, B.F., REED, C.B., WALKER, J.S. (1989) *Fusion Engng Design*, **8**, 241-248.
[9] TALMAGE, G., WALKER, J.S. (1988) *Beer Sheva Conference*, 3-25.
[10] REED, C.B., PICOLOGLOU, B.F., HUA, T.Q., WALKER, J.S. (1987) *IEEE No. 87CH2507-2*, 1267-1270.
[11] REED, C.B. et al (1995) *Fusion Engng Design*, **27**, 614-626.
[12] BÜHLER, L. (1995) *Fusion Technology* **27**, 3-24.
[13] MOLOKOV, S., REED, C.B. (2001) *Argonne National Laboratory Report, ANL/TD/TM01-18*.
[14] MOLOKOV, S., REED, C.B. (2002) Parametric study of the liquid metal flow in a straight insulated circular duct in a strong nonuniform magnetic field, *Fusion Science and Technology (to be published).*
[15] MOLOKOV, S., REED, C.B. (2001) *Argonne National Laboratory Report, ANL/TD/TM01-19*.
[16] LIELAUSIS, O. (1975) *Atomic Energy Review*, **13**, 527-581.
[17] MOREA U, R. (1990) *Magnetohydrodynamics, Kluwer*.
[18] MÜLLER, U., BÜHLER, L. (2001) *Magnetofluiddynamics in channels and containers, Springer*.
[19] KIRILLOV, I.R., REED, C.B., BARLEON, L., MIYAZAKI, K. (1995) *Fusion Engng Design*, **27**, 553-569.
[20] ALEKSANDROVA, S., MOLOKOV, S., REED, C.B. (2002) *Argonne National Laboratory Report, ANL/TD/TM02-30*.
[21] REED, C.B. PICOLOGLOU, B. F. DAUZVARDIS P. V. (1985) *Experimental Facility for Studying MHD Effects in Liquid Metal Cooled Blankets, Fusion Technology, **8**, 257-268*